Azimuthal Anisotropy of Heavy-Flavor Decay Electrons in p-Pb Collisions at √sNN = 5.02 TeV

(ALICE Collaboration) Acharya, S.; ...; Antičić, Tome; ...; Erhardt, Filip; ...; Gotovac, Sven; ...; Jerčić, Marko; ...; ...

Journal article, Published version
Rad u časopisu, Objavljena verzija rada (izdavačev PDF)

Permanent link / Trajna poveznica: https://urn.nsk.hr/urn:nbn:hr:217:244386

Download date / Datum preuzimanja: **2024-10-05**

Azimuthal Anisotropy of Heavy-Flavor Decay Electrons in p-Pb Collisions at $\sqrt{s_{NN}} = 5.02$ TeV

S. Acharya *et al.*[*]

(ALICE Collaboration)

Angular correlations between heavy-flavor decay electrons and charged particles at midrapidity ($|\eta| < 0.8$) are measured in p-Pb collisions at $\sqrt{s_{NN}} = 5.02$ TeV. The analysis is carried out for the 0%–20% (high) and 60%–100% (low) multiplicity ranges. The jet contribution in the correlation distribution from high-multiplicity events is removed by subtracting the distribution from low-multiplicity events. An azimuthal modulation remains after removing the jet contribution, similar to previous observations in two-particle angular correlation measurements for light-flavor hadrons. A Fourier decomposition of the modulation results in a positive second-order coefficient (v_2) for heavy-flavor decay electrons in the transverse momentum interval $1.5 < p_T < 4$ GeV/c in high-multiplicity events, with a significance larger than 5σ. The results are compared with those of charged particles at midrapidity and those of inclusive muons at forward rapidity. The v_2 measurement of open heavy-flavor particles at midrapidity in small collision systems could provide crucial information to help interpret the anisotropies observed in such systems.

Two-particle angular correlations are a powerful tool to study the dynamical evolution of the system created in ultrarelativistic collisions of protons or nuclei. The differences in the azimuthal angle ($\Delta\varphi$) and in pseudorapidity ($\Delta\eta$) between a reference ("trigger") particle and other particles produced in the event are considered. The typical shape of the correlation distribution features a near-side peak at $(\Delta\varphi, \Delta\eta) \sim (0,0)$, originating from cases in which the trigger particle is produced in a jet, and an away-side structure centered at $\Delta\varphi \sim \pi$ and extending over a wide pseudorapidity range, due to the recoil jet [1]. In nucleus-nucleus collisions, the correlation distribution also exhibits pronounced structures on the near and away sides extending over a large $\Delta\eta$ region, commonly referred to as "ridges" [2]. They can be quantified by the $V_{n\Delta}$ coefficient of a Fourier decomposition of the $\Delta\varphi$ distribution, which is performed after removing the jet contribution. These coefficients can be factorized into single-particle coefficients v_n related to the azimuthal distribution of the particles with respect to the nth-order symmetry planes [3]. In noncentral nucleus-nucleus collisions, the dominant coefficient is that of the second-order harmonic, referred to as elliptic flow (v_2), and its value is used to characterize the collective motion of the system. The measurements are well

described by models invoking a hydrodynamic expansion of the hot and dense medium produced in the collision. This translates the initial-state spatial anisotropy, due to the asymmetry of the nuclear overlap region, into a momentum anisotropy of the particles emerging from the medium [4]. This collective motion is one of the important features of the quark-gluon plasma (QGP) produced in such collisions.

Surprisingly, the presence of similar long-range ridge structures and a positive v_2 coefficient were also observed for light-flavor hadrons in high-multiplicity proton-lead (p-Pb) collisions by the ALICE [5], ATLAS [6], and CMS [7] Collaborations at the LHC. The pattern of the v_2 coefficient as a function of the particle mass and transverse momentum is similar in p-Pb and Pb-Pb collisions [8,9]. The PHENIX and STAR Collaborations at RHIC also measured a positive v_2 coefficient for charged hadrons in high-multiplicity d-Au and ^{3}He-Au collisions [10–12]. A near-side structure extended over a large $\Delta\eta$ range was also reported for high-multiplicity proton-proton (pp) collisions by the CMS [13] and ATLAS [6] Collaborations. The interpretation of a positive v_2 in these small collision systems is currently highly debated [14]. One possible interpretation is based on collective effects induced by a hydrodynamical evolution of the particles produced in the collision [15,16]. Other approaches include mechanisms involving initial-state effects, such as gluon saturation within the color-glass condensate effective field theory [17,18], or final-state color-charge exchanges [19,20].

Because of their large masses, heavy quarks are produced in hard scattering processes during the early stages of hadronic collisions [21]. In heavy-ion collisions, the elliptic

---

[*]Full author list given at the end of the article.

flow of charm mesons [22–25] and heavy-flavor decay leptons [26–30] was found to have similar magnitude to that of charged particles [31], dominated by light-flavor hadrons. A search for a nonzero v_2 in the correlation pattern of heavy-flavor particles in high-multiplicity p-Pb collisions could provide further insight on the initial- and final-state origin of the anisotropies in this collision system, helping in constraining the models that describe the ridge structures. The production mechanisms of heavy quarks, involving a large squared four-momentum transfer, are also different from those of light-flavor quarks. This creates the possibility to investigate whether the onset of the anisotropy of the particle azimuthal distribution is affected by the details of hard scattering and fragmentation processes.

In this Letter, we present the measurement of v_2 for open heavy-flavor particles at midrapidity in high-multiplicity p-Pb collisions at $\sqrt{s_{NN}} = 5.02$ TeV via azimuthal correlations of electrons from charm and beauty hadron decays, and charged particles. This result complements our previous studies of hidden charm particles based on the measurement of the correlations between J/ψ mesons at forward rapidity and charged particles at midrapidity in high-multiplicity p-Pb collisions at $\sqrt{s_{NN}} = 5.02$ TeV and 8.16 TeV, which found evidences for a positive v_2 of J/ψ mesons [32]. A positive v_2 of muons at forward and backward rapidity, which are predominantly produced by heavy-flavor decays for transverse momentum (p_T) greater than 2 GeV/c, was also measured in high-multiplicity p-Pb collisions at $\sqrt{s_{NN}} = 5.02$ TeV [33]. Similar indications of positive v_2 were also reported at midrapidity in high-multiplicity p-Pb collisions at $\sqrt{s_{NN}} = 8.16$ TeV for D^0 mesons by the CMS Collaboration [34] and in preliminary results for D^{*+} mesons [35] and heavy-flavor decay muons [36] by the ATLAS Collaboration.

The data sample used for the analysis was collected by the ALICE experiment [37,38] in 2016 during the LHC p-Pb run at $\sqrt{s_{NN}} = 5.02$ TeV. The center-of-mass reference frame of the nucleon-nucleon collision was shifted in rapidity by 0.465 units in the proton-going direction with respect to the laboratory frame. The events were recorded using a minimum-bias trigger, which required coincident signals in the two scintillator arrays of the V0 detector, covering the full azimuthal angle in the pseudorapidity (η) ranges $2.8 < \eta < 5.1$ (V0-A) and $-3.7 < \eta < -1.7$ (V0-C). Together with the V0 information, signals from the two Zero-Degree Calorimeters were used to reject the beam-induced background. Only events with a primary vertex reconstructed within ± 10 cm from the center of the detector along the beam axis were accepted. About 6×10^8 events, corresponding to an integrated luminosity of $L_{\rm int} = 295 \pm 11$ μb^{-1}, were obtained after these selections. Only events in high- (0%–20%) and low-multiplicity (60%–100%) classes, evaluated using the signal amplitude in the V0-A detector [39], were considered.

Electrons with transverse momentum (p_T^e) in the interval $1.5 < p_T^e < 6$ GeV/c and $|\eta| < 0.8$ (corresponding to $-1.26 < y_{\rm cms}^e < 0.34$, where $y_{\rm cms}^e$ is the electron rapidity in the center-of-mass reference frame) were selected using similar criteria as discussed in Ref. [40]. Charged tracks were reconstructed using the Inner Tracking System (ITS), comprising six layers of silicon detectors with the innermost two composed of pixel detectors, and the Time Projection Chamber (TPC), a gaseous detector and the main tracking device. Tracks were required to have hits on both pixel layers of the ITS and a distance of closest approach to the primary vertex of less than 1 cm along the beam axis and 0.25 cm in the transverse plane, to reduce the contamination of electrons from photon conversions and particle weak decays [41]. The particle identification employed a selection on the specific ionization energy loss inside the TPC of $-1 < n_\sigma^{\rm TPC} < 3$, where n_σ is the difference between the measured and expected detector response signals for electrons normalized to the response resolution. A selection ($-3 < n_\sigma^{\rm TOF} < 3$) was also applied using the Time of Flight (TOF) detector to further separate hadrons and electrons. The electron reconstruction efficiency was calculated using Monte Carlo simulations of events containing $c\bar{c}$ and $b\bar{b}$ pairs generated with PYTHIA 6.4.21 [42] and the Perugia-2011 tune [43], and an underlying p-Pb collision generated using HIJING 1.36 [44]. The generated particles were propagated through the detector using the GEANT3 transport package [45]. With the selections described above, the resulting electron reconstruction efficiency is about 28% (32%) at $p_T^e = 1.5$ GeV/c (6 GeV/c). The contamination from charged hadrons, estimated as described in Ref. [46], amounts to about 1% (10%) for $1.5 < p_T^e < 4$ GeV/c ($4 < p_T^e < 6$ GeV/c).

The selected electrons are composed of signal heavy-flavor decay electrons (HFe), originating from semileptonic decays of open heavy-flavor hadrons, and background electrons. The main background sources are photon conversions ($\gamma \rightarrow e^+ e^-$) in the beam vacuum tube, and in the material of the innermost ITS layers, and Dalitz decays of neutral mesons ($\pi^0 \rightarrow \gamma e^+ e^-$ and $\eta \rightarrow \gamma e^+ e^-$), defined as non-heavy-flavor decay electrons (NonHFe) hereafter. Background contributions from other Dalitz decays, or decays of kaons and J/ψ mesons, are negligible in the p_T range studied in the analysis [40] and were not considered. To estimate the background contribution, dielectron pairs were defined by pairing the selected electrons with opposite-charge electron partners to form unlike-signed pairs (ULS) and calculating their invariant mass ($M_{e^+ e^-}$). Partner electrons were selected, applying similar but looser track quality and particle identification criteria than those used for selecting signal electrons. The dielectron pairs from NonHFe sources have a small invariant mass, while heavy-flavor decay electrons can form ULS pairs mainly through random combinations with other electrons, resulting in a continuous invariant-mass distribution. The

combinatorial contribution was estimated from the invariant-mass distribution of like-signed (LS) electron pairs. The NonHFe background contribution was then evaluated by subtracting the LS distribution from the ULS distribution in the invariant-mass region $M_{e^+e^-} < 140$ MeV/c^2. More details on the procedure can be found in Refs. [40,47]. The efficiency ($\varepsilon_{\mathrm{NonHF}e}$) of finding the partner electron to identify non-heavy-flavor decay electrons was calculated with the aforementioned Monte Carlo simulations, and is about 60% for $1.5 < p_T^e < 2$ GeV/c, rising to 76% for $4 < p_T^e < 6$ GeV/c.

The number of heavy-flavor decay electrons ($N_{\mathrm{HF}e}$) can be expressed as

$$N_{\mathrm{HF}e} = N_e - N_{\mathrm{NonHF}e} = N_e - \frac{1}{\varepsilon_{\mathrm{NonHF}e}}(N_{\mathrm{ULS}e} - N_{\mathrm{LS}e}), \quad (1)$$

where $N_{\mathrm{ULS}e}$ and $N_{\mathrm{LS}e}$ are the number of electrons which form unlike-sign and like-sign pairs, respectively, with $M_{e^+e^-} < 140$ MeV/c^2, and N_e is the number of selected electrons.

The two-particle correlation distributions between electrons (trigger) and charged (associated) particles were obtained for three different p_T^e intervals ($1.5 < p_T^e < 2$ GeV/c, $2 < p_T^e < 4$ GeV/c, and $4 < p_T^e < 6$ GeV/c). Associated charged particles with $0.3 < p_T^{\mathrm{ch}} < 2$ GeV/c and $|\eta| < 0.8$ were selected with similar criteria as used for electrons, apart from requiring a hit in at least one, instead of both, of the two pixel layers and not applying any particle identification. The single-track reconstruction efficiency and the contamination from secondary particles [41] were estimated using Monte Carlo simulations of p-Pb collisions produced with the DPMJET 3.0 event generator [48] and GEANT3 [45] for the particle transport. Both were found to be independent of the event multiplicity. With the selections described above, the tracking efficiency varies from 75% to 85% depending on track momentum and primary vertex position, and the contamination of secondary particles varies from 3% to 5.5% with decreasing p_T^{ch}.

The $(\Delta\varphi, \Delta\eta)$ correlation distribution between heavy-flavor decay electrons and charged particles is obtained with the equation

$$\begin{aligned} S_{\mathrm{HF}e} &= S_e - S_{\mathrm{NonHF}e} \\ &= S_e - S_{\mathrm{NonHF}e}^{\mathrm{ID}} - S_{\mathrm{NonHF}e}^{\mathrm{nonID}} \\ &= S_e - S_{\mathrm{NonHF}e}^{\mathrm{ID}} - \left(\frac{1}{\varepsilon_{\mathrm{NonHF}e}} - 1\right) S_{\mathrm{NonHF}e}^{\mathrm{ID*}}, \quad (2) \end{aligned}$$

where S corresponds to $d^2N_{e\text{-}\mathrm{ch}}(\Delta\eta, \Delta\varphi)/d\Delta\eta d\Delta\varphi$. The correlation distributions for all trigger electrons and for non-heavy-flavor decay trigger electrons are denoted as S_e and $S_{\mathrm{NonHF}e}$, respectively. The hadron contamination in S_e is statistically removed by subtracting a scaled dihadron correlation distribution. The $S_{\mathrm{NonHF}e}$ distribution is

evaluated from its two contributions $S_{\mathrm{NonHF}e}^{\mathrm{ID}}$ and $S_{\mathrm{NonHF}e}^{\mathrm{nonID}}$. The former corresponds to correlations from background electron triggers with an identified electron partner, and the latter to the expected contribution from background trigger electrons without an identified partner. The identified background distribution, $S_{\mathrm{NonHF}e}^{\mathrm{ID}}$, is evaluated using correlations of trigger electrons paired with unlike-sign and like-sign electrons, with a similar procedure as that used to evaluate $N_{\mathrm{NonHF}e}$ [see Eq. (1)]. The nonidentified distribution, $S_{\mathrm{NonHF}e}^{\mathrm{nonID}}$, is estimated assuming that both identified and nonidentified NonHFe triggers have the same correlation distribution, apart from reconstructed partner electrons used to calculate $M_{e^+e^-}$, which are removed from $S_{\mathrm{NonHF}e}^{\mathrm{ID}}$ to obtain $S_{\mathrm{NonHF}e}^{\mathrm{ID*}}$.

The correlation distribution for heavy-flavor decay electrons was corrected for the electron and charged particle reconstruction efficiencies and for the secondary particle contamination. It was also corrected for the limited two-particle acceptance and detector inhomogeneities using the event mixing technique [8]. The mixed-event correlation distribution was obtained by combining electrons in an event with charged particles from other events with similar multiplicity and primary vertex position. The correlation distribution for heavy-flavor decay electrons was divided by the number of heavy-flavor decay trigger electrons [$N_{\mathrm{HF}e}$, from Eq. (1)] corrected by their reconstruction efficiency.

The two-dimensional correlation distribution was projected onto $\Delta\varphi$ for $|\Delta\eta| < 1.2$ and divided by the width of the selected $\Delta\eta$ interval. A baseline term, constant in $\Delta\varphi$, was subtracted from the correlation distributions. Its values, reported in Table I, were calculated as the weighted average of the three lowest points of the distribution, following the "zero yield at minimum" approach [49]. The resulting correlation distributions in the two considered multiplicity classes (0%–20% and 60%–100%) are shown in Fig. 1 for $2 < p_T^e < 4$ GeV/c. An enhancement of the near- and away-side peaks is present in high-multiplicity collisions. To study this feature, the baseline-subtracted correlation distribution obtained in low-multiplicity events was subtracted from the correlation distribution measured in high-multiplicity events, as described in Ref. [5]. This removes the jet-induced correlation peaks, assuming that they are the same in low- and high-multiplicity events. The correlation distribution was restricted to the $(0, \pi)$ range by reflecting the symmetrical points. The resulting distribution, shown in Fig. 2, was fitted with the Fourier decomposition of Eq. (3). An azimuthal anisotropy, dominated by the second-order term $V_{2\Delta}^{\mathrm{HF}e\text{-}\mathrm{ch}}$, was found.

$$\begin{aligned} \frac{1}{\Delta\eta} & \frac{1}{N_{\mathrm{HF}e}} \frac{dN_{\mathrm{HF}e\text{-}\mathrm{ch}}(\Delta\varphi)}{d\Delta\varphi} \\ &= a[1 + 2V_{1\Delta}^{\mathrm{HF}e\text{-}\mathrm{ch}}\cos(\Delta\varphi) + 2V_{2\Delta}^{\mathrm{HF}e\text{-}\mathrm{ch}}\cos(2\Delta\varphi)] \quad (3) \end{aligned}$$

TABLE I.   Results for $V_{2\Delta}^{\mathrm{HF}e\text{-ch}}$ and baselines in high- (b_{HM}) and low-multiplicity (b_{LM}) collisions.

p_T^e (GeV/c)	$V_{2\Delta}^{\mathrm{HF}e\text{-ch}} \pm$ stat $\pm$ syst	$b_{\mathrm{LM}} \pm$ stat $\pm$ syst (rad^{-1})	$b_{\mathrm{HM}} \pm$ stat $\pm$ syst (rad^{-1})
$1.5 < p_T^e < 2$	$(38 \pm 8 \pm 6) \times 10^{-4}$	$1.235 \pm 0.006 \pm 0.037$	$4.312 \pm 0.008 \pm 0.129$
$2 < p_T^e < 4$	$(40 \pm 7 \pm 5) \times 10^{-4}$	$1.294 \pm 0.008 \pm 0.038$	$4.330 \pm 0.007 \pm 0.129$
$4 < p_T^e < 6$	$(19 \pm 19 \pm 3) \times 10^{-4}$	$1.433 \pm 0.022 \pm 0.043$	$4.754 \pm 0.020 \pm 0.142$

The measured $V_{2\Delta}^{\mathrm{HF}e\text{-ch}}$ in high-multiplicity events does not exclude the possibility of having a $V_{2\Delta}^{\mathrm{HF}e\text{-ch}}$ contribution in the low-multiplicity events, as described in Ref. [6].

The systematic uncertainties on the azimuthal correlation distribution can originate from (i) potential biases in the procedure employed to select electron candidates and estimate the hadron contamination, (ii) removal of the background electrons not produced in heavy-flavor hadron decays, and (iii) choice of the associated particle selection. A systematic uncertainty related to the electron reconstruction efficiency arises from imprecisions in the description of the detector response. It was studied by varying the electron selection in the ITS and TPC. The uncertainty affecting the removal of the hadron contamination was estimated by varying the particle identification criteria in the TPC (n_σ^{TPC}). A total uncertainty of less than 0.5% was estimated from these sources. The uncertainty related to the efficiency of finding the partner electron and to the stability of the $S_{\mathrm{NonHF}e}$ distribution was studied by varying the selection for partner tracks and pair invariant mass, resulting in an uncertainty of less than 0.5%. The uncertainty on the associated track reconstruction efficiency, obtained by varying the associated track selection criteria and by comparing the probabilities of track prolongation from TPC to ITS in data and simulations, was estimated to be 3% [50]. A systematic effect due to the contamination of the associated particles by secondaries comes from residual
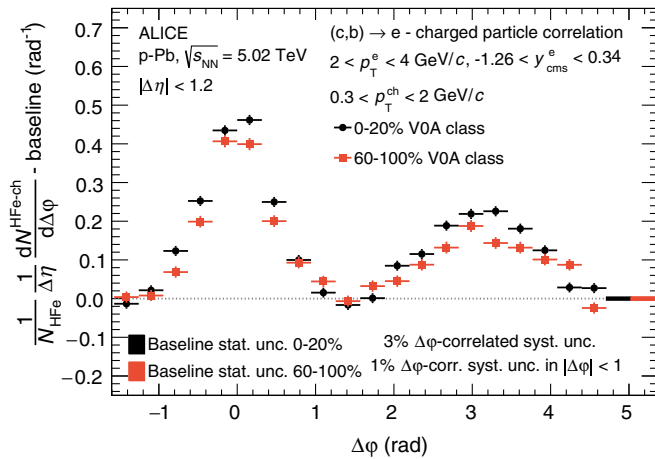
discrepancy between Monte Carlo simulations and data in the relative abundances of particle species and was studied by varying the selection on the distance of closest approach to the primary vertex. It was quantified to be 1% (correlated in $\Delta\varphi$), with an additional 1% (correlated) for $|\Delta\varphi| < 1$. Combining the uncertainties from all the above sources results in a 3% total systematic uncertainty (correlated in $\Delta\varphi$) and an additional 1% (also correlated) for $|\Delta\varphi| < 1$.

The systematic uncertainties from the above mentioned sources are also present in the $V_{2\Delta}^{\mathrm{HF}e\text{-ch}}$. The uncertainty related to the electron selection and the identification of non-heavy-flavor decay electrons on $V_{2\Delta}^{\mathrm{HF}e\text{-ch}}$ were quantified to be about 2%–3% and 5%, respectively. The contamination of the associated particles by secondaries leads to a 3% systematic uncertainty. In order to test whether the observed $\Delta\varphi$ modulation and the nonzero $V_{2\Delta}^{\mathrm{HF}e\text{-ch}}$ could originate from a residual jet contribution, due to possible differences between the jet structures in low- and high-multiplicity collisions, the $\Delta\eta$ integration region was modified by excluding central intervals of $|\Delta\eta| < \Delta\eta^{\mathrm{gap}}$, varying $\Delta\eta^{\mathrm{gap}}$ from 0.2 to 0.6. The observed variation on $V_{2\Delta}^{\mathrm{HF}e\text{-ch}}$ was 11%–15%, depending on the electron p_T interval, and was taken as the systematic uncertainty from the jet subtraction. The stability of the

FIG. 1.   Azimuthal correlations between heavy-flavor decay electrons and charged particles, for high-multiplicity and low-multiplicity p-Pb collisions, after subtracting the baseline (see text for details) for $2 < p_T^e < 4$ GeV/c and $0.3 < p_T^{\mathrm{ch}} < 2$ GeV/c.
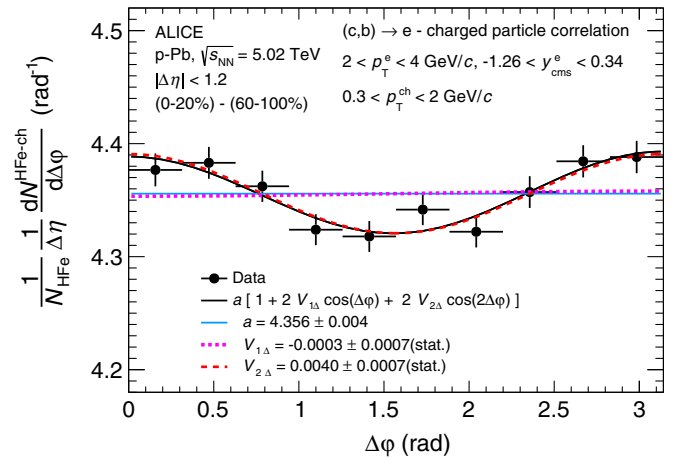

FIG. 2.   Best fit [Eq. (3)] to the azimuthal correlation distribution between heavy-flavor decay electrons and charged particles, for high-multiplicity p-Pb collisions after subtracting the jet contribution based on low-multiplicity collisions. The distribution is shown for $2 < p_T^e < 4$ GeV/c and $0.3 < p_T^{\mathrm{ch}} < 2$ GeV/c. The figure shows only statistical uncertainty.

$V_{2\Delta}^{\mathrm{HF}e\text{-ch}}$ value against the variation of the $\Delta\eta$ range suggests a long-range nature of the observed anisotropy. The inclusion of a $V_{3\Delta}^{\mathrm{HF}e\text{-ch}}$ term in the fit function, in Eq. (3), affects the $V_{2\Delta}^{\mathrm{HF}e\text{-ch}}$ estimation by less than 0.5%. Combining the different uncertainty sources results in a total systematic uncertainty on $V_{2\Delta}^{\mathrm{HF}e\text{-ch}}$ of 13%–16% depending on p_T^e.

The values of $V_{2\Delta}^{\mathrm{HF}e\text{-ch}}$ obtained from the fits are reported in Table I. The measured $V_{2\Delta}^{\mathrm{HF}e\text{-ch}}$ is larger than zero with a significance of 4.6σ for the $2 < p_T^e < 4$ GeV/c range. The significance for $V_{2\Delta}^{\mathrm{HF}e\text{-ch}} > 0$ in the interval $1.5 < p_T^e < 4$ GeV/c, considering statistical and systematic uncertainties, is about 6σ.

Assuming its factorization in single-particle v_2 coefficients [8], $V_{2\Delta}^{\mathrm{HF}e\text{-ch}}$ can be expressed as the product of the second-order Fourier coefficients of the heavy-flavor decay electron ($v_2^{\mathrm{HF}e}$) and charged particle (v_2^{ch}) azimuthal distributions, hence $v_2^{\mathrm{HF}e} = V_{2\Delta}^{\mathrm{HF}e\text{-ch}}/v_2^{\mathrm{ch}}$. The v_2^{ch} value in the range $0.3 < p_T^{\mathrm{ch}} < 2$ GeV/c was obtained from the weighted average of the values measured in smaller p_T^{ch} ranges in Ref. [8], providing $v_2^{\mathrm{ch}} = 0.0594 \pm 0.0010(\text{stat}) \pm 0.0059(\text{syst})$. The obtained $v_2^{\mathrm{HF}e}$ values are reported in Fig. 3 and compared to v_2 of charged particles, dominated by light-flavor hadrons, and to inclusive muons at large rapidity, mostly originating from heavy-flavor hadron decays for $p_T^{\mu} > 2$ GeV/c. The heavy-flavor decay electron v_2 is lower than v_2^{ch}, though the uncertainties are large, and the p_T interval of electron parents (heavy-flavor hadrons) is considerably broader than the range addressed in the light-flavor hadron measurement. The v_2 values for heavy-flavor electrons and inclusive muons are similar, although a direct comparison is not straightforward, given the different rapidities and the contamination in the muon sample for $p_T^{\mu} < 2$ GeV/c. The $v_2^{\mathrm{HF}e}$ in p-Pb collisions has similar magnitude to that measured in noncentral Pb-Pb collisions at $\sqrt{s_{NN}} = 2.76$ TeV [29]. The significance for

$v_2^{\mathrm{HF}e} > 0$ is 5.1σ for $1.5 < p_T^e < 4$ GeV/c, providing very strong indications for the presence of long-range anisotropies for heavy-flavor particles in high-multiplicity p-Pb collisions.

In summary, we report the measurement of v_2 for open heavy-flavor particles at midrapidity in high-multiplicity p-Pb collisions. The analysis was carried out via a Fourier decomposition of the azimuthal correlation distribution between heavy-flavor decay electrons and charged particles. After removing the jet contribution and fitting the high-multiplicity correlation distributions, a $V_{2\Delta}$-like modulation was obtained, qualitatively similar to the one observed for charged particles [5]. The measured heavy-flavor decay electron v_2 is positive with a significance of more than 5σ in the $1.5 < p_T^e < 4$ GeV/c range. Its values are possibly lower than charged particle v_2 [5], and similar to inclusive muon v_2 at large rapidity [33]. Complementing previous results for light-flavor hadrons [5], this measurement provides new information on the behavior of heavy-flavor hadrons to understand the azimuthal anisotropies observed in small collision systems.
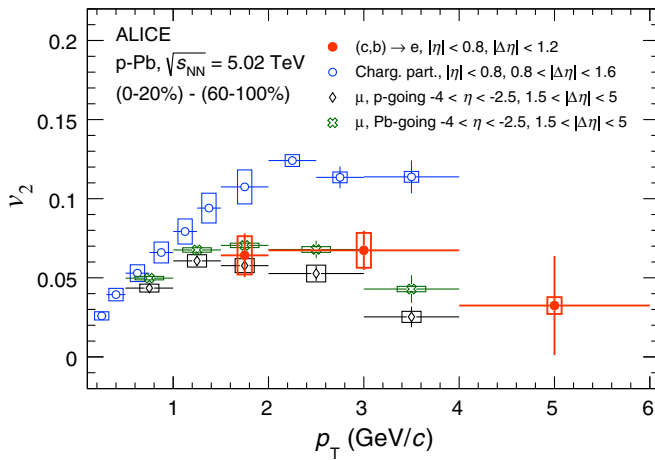
FIG. 3. Heavy-flavor decay electron v_2 as a function of transverse momentum compared to the v_2 of unidentified charged particles [8] and inclusive muons [33].

---

[1] X.-N. Wang, Studying mini-jets via the p_T dependence of the two particle correlation in azimuthal angle φ, Phys. Rev. D **47**, 2754 (1993).

[2] B. I. Abelev *et al.* (STAR Collaboration), Long range rapidity correlations and jet production in high energy nuclear collisions, Phys. Rev. C **80**, 064912 (2009).

[3] K. Aamodt *et al.* (ALICE Collaboration), Harmonic decomposition of two-particle angular correlations in Pb-Pb collisions at $\sqrt{s_{NN}} = 2.76$ TeV, Phys. Lett. B **708**, 249 (2012).

[4] G.-Y. Qin, H. Petersen, S. A. Bass, and B. Muller, Translation of collision geometry fluctuations into momentum anisotropies in relativistic heavy-ion collisions, Phys. Rev. C **82**, 064903 (2010).

[5] B. Abelev *et al.* (ALICE Collaboration), Long-range angular correlations on the near and away side in p-Pb collisions at $\sqrt{s_{NN}} = 5.02$ TeV, Phys. Lett. B **719**, 29 (2013).

[6] M. Aaboud *et al.* (ATLAS Collaboration), Measurements of long-range azimuthal anisotropies and associated Fourier coefficients for pp collisions at $\sqrt{s} = 5.02$ and 13 TeV and $p + $Pb collisions at $\sqrt{s_{NN}} = 5.02$ TeV with the ATLAS detector, Phys. Rev. C **96**, 024908 (2017).

[7] S. Chatrchyan *et al.* (CMS Collaboration), Multiplicity and transverse momentum dependence of two- and four-particle correlations in p-Pb and Pb-Pb collisions, Phys. Lett. B **724**, 213 (2013).

[8] B. Abelev *et al.* (ALICE Collaboration), Long-range angular correlations of π, K, and p in p-Pb collisions at $\sqrt{s_{NN}} = 5.02$ TeV, Phys. Lett. B **726**, 164 (2013).

[9] V. Khachatryan *et al.* (CMS Collaboration), Long-range two-particle correlations of strange hadrons with charged particles in p-Pb and Pb-Pb collisions at LHC energies, Phys. Lett. B **742**, 200 (2015).

[10] A. Adare *et al.* (PHENIX Collaboration), Quadrupole Anisotropy in Dihadron Azimuthal Correlations in Central $d + $Au Collisions at $\sqrt{s_{NN}} = 200$ GeV, Phys. Rev. Lett. **111**, 212301 (2013).

[11] L. Adamczyk *et al.* (STAR Collaboration), Long-range pseudorapidity dihadron correlations in $d + $Au collisions at $\sqrt{s_{NN}} = 200$ GeV, Phys. Lett. B **747**, 265 (2015).

[12] A. Adare *et al.* (PHENIX Collaboration), Measurements of Elliptic and Triangular Flow in High-Multiplicity ^{3}He $+$ Au Collisions at $\sqrt{s_{NN}} = 200$ GeV, Phys. Rev. Lett. **115**, 142301 (2015).

[13] V. Khachatryan *et al.* (CMS Collaboration), Observation of long-range near-side angular correlations in proton-proton collisions at the LHC, J. High Energy Phys. 09 (2010) 091.

[14] C. Loizides, Experimental overview on small collision systems at the LHC, Nucl. Phys. **A956**, 200 (2016).

[15] K. Werner, I. Karpenko, and T. Pierog, The "Ridge" in Proton-Proton Scattering at 7 TeV, Phys. Rev. Lett. 106, 122004 (2011).

[16] W.-T. Deng, Z. Xu, and C. Greiner, Elliptic and triangular flow and their correlation in ultrarelativistic high multiplicity proton proton collisions at 14 TeV, Phys. Lett. B 711, 301 (2012).

[17] K. Dusling and R. Venugopalan, Comparison of the color glass condensate to dihadron correlations in proton-proton and proton-nucleus collisions, Phys. Rev. D 87, 094034 (2013).

[18] A. Bzdak, B. Schenke, P. Tribedy, and R. Venugopalan, Initial state geometry and the role of hydrodynamics in proton-proton, proton-nucleus and deuteron-nucleus collisions, Phys. Rev. C 87, 064906 (2013).

[19] A. Dumitru, T. Lappi, and L. McLerran, Are the angular correlations in pA collisions due to a Glasmion or Bose condensation?, Nucl. Phys. A922, 140 (2014).

[20] C.-Y. Wong, Momentum kick model description of the ridge in $\Delta\phi - \Delta\eta$ correlation in pp collisions at 7 TeV, Phys. Rev. C 84, 024901 (2011).

[21] A. Andronic et al., Heavy-flavour and quarkonium production in the LHC era: From protonproton to heavy-ion collisions, Eur. Phys. J. C 76, 107 (2016).

[22] L. Adamczyk et al. (STAR Collaboration), Measurement of D^0 Azimuthal Anisotropy at Midrapidity in Au + Au Collisions at $\sqrt{s_{NN}} = 200$ GeV, Phys. Rev. Lett. 118, 212301 (2017).

[23] S. Acharya et al. (ALICE Collaboration), D-meson Azimuthal Anisotropy in Midcentral Pb-Pb Collisions at $\sqrt{s_{NN}} = 5.02$ TeV, Phys. Rev. Lett. 120, 102301 (2018).

[24] B. Abelev et al. (ALICE Collaboration), Azimuthal anisotropy of D meson production in Pb-Pb collisions at $\sqrt{s_{NN}} = 2.76$ TeV, Phys. Rev. C 90, 034904 (2014).

[25] A. M. Sirunyan et al. (CMS Collaboration), Measurement of Prompt D^0 Meson Azimuthal Anisotropy in Pb-Pb Collisions at $\sqrt{s_{NN}} = 5.02$ TeV, Phys. Rev. Lett. 120, 202301 (2018).

[26] A. Adare et al. (PHENIX Collaboration), Heavy quark production in $p + p$ and energy loss and flow of heavy quarks in Au + Au collisions at $\sqrt{s_{NN}} = 200$ GeV, Phys. Rev. C 84, 044905 (2011).

[27] L. Adamczyk et al. (STAR Collaboration), Elliptic flow of electrons from heavy-flavor hadron decays in Au + Au collisions at $\sqrt{s_{NN}} = 200$, 62.4, and 39 GeV, Phys. Rev. C 95, 034907 (2017).

[28] J. Adam et al. (ALICE Collaboration), Elliptic flow of muons from heavy-flavour hadron decays at forward rapidity in Pb-Pb collisions at $\sqrt{s_{NN}} = 2.76$ TeV, Phys. Lett. B 753, 41 (2016).

[29] J. Adam et al. (ALICE Collaboration), Elliptic flow of electrons from heavy-flavour hadron decays at mid-rapidity in Pb-Pb collisions at $\sqrt{s_{NN}} = 2.76$ TeV, J. High Energy Phys. 09 (2016) 028.

[30] M. Aaboud et al. (ATLAS Collaboration), Measurement of the suppression and azimuthal anisotropy of muons from heavy-flavor decays in Pb + Pb collisions at $\sqrt{s_{NN}} = 2.76$ TeV with the ATLAS detector, Phys. Rev. C 98, 044905 (2018).

[31] B. Abelev et al. (ALICE Collaboration), Anisotropic flow of charged hadrons, pions and (anti)protons measured at high transverse momentum in Pb-Pb collisions at $\sqrt{s_{NN}} = 2.76$ TeV, Phys. Lett. B 719, 18 (2013).

[32] S. Acharya et al. (ALICE Collaboration), Search for collectivity with azimuthal J/ψ-hadron correlations in high multiplicity p-Pb collisions at $\sqrt{s_{NN}} = 5.02$ and 8.16 TeV, Phys. Lett. B 780, 7 (2018).

[33] J. Adam et al. (ALICE Collaboration), Forward-central two-particle correlations in p-Pb collisions at $\sqrt{s_{NN}} = 5.02$ TeV, Phys. Lett. B 753, 126 (2016).

[34] A. M. Sirunyan et al. (CMS Collaboration), Elliptic Flow of Charm and Strange Hadrons in High-Multiplicity p-Pb Collisions at $\sqrt{s_{NN}} = 8.16$ TeV, Phys. Rev. Lett. 121, 082301 (2018).

[35] ATLAS Collaboration, D-meson production and long-range azimuthal correlation in 8.16 TeV $p + Pb$ collisions with ATLAS, Technical Report No. ATLAS-CONF-2017-073, CERN, Geneva, 2017.

[36] ATLAS Collaboration, Measurement of the long-range pseudorapidity correlations between muons and charged particles in $\sqrt{s_{NN}} = 8.16$ TeV proton-lead collisions with the ATLAS detector, Technical Report No. ATLAS-CONF-2017-006, CERN, Geneva, 2017.

[37] K. Aamodt et al. (ALICE Collaboration), The ALICE experiment at the CERN LHC, J. Instrum. 3, S08002 (2008).

[38] B. Abelev et al. (ALICE Collaboration), Performance of the ALICE Experiment at the CERN LHC, Int. J. Mod. Phys. A 29, 1430044 (2014).

[39] J. Adam et al. (ALICE Collaboration), Centrality dependence of particle production in p-Pb collisions at $\sqrt{s_{NN}} = 5.02$ TeV, Phys. Rev. C 91, 064905 (2015).

[40] J. Adam et al. (ALICE Collaboration), Measurement of electrons from heavy-flavour hadron decays in p-Pb collisions at $\sqrt{s_{NN}} = 5.02$ TeV, Phys. Lett. B 754, 81 (2016).

[41] ALICE Collaboration, The ALICE definition of primary particles. https://cds.cern.ch/record/2270008.

[42] T. Sjostrand, S. Mrenna, and P. Z. Skands, PYTHIA 6.4 physics and manual, J. High Energy Phys. 05 (2006) 026.

[43] P. Z. Skands, The perugia tunes, in Proceedings, 1st International Workshop on Multiple Partonic Interactions at the LHC (MPI08): Perugia, Italy, 2008 (Verlag Deutsches Elektronen-Synchrotron, Hamburg, 2009), pp. 284–297.

[44] X.-N. Wang and M. Gyulassy, HIJING: A Monte Carlo model for multiple jet production in pp, pA and AA collisions, Phys. Rev. D 44, 3501 (1991).

[45] Rene Brun et al., GEANT Detector Description and Simulation Tool, CERN Program Library, Long Write-up, W5013 (CERN, Geneva, 1994).

[46] B. Abelev et al. (ALICE Collaboration), Measurement of electrons from semileptonic heavy-flavour hadron decays in pp collisions at $\sqrt{s} = 7$ TeV, Phys. Rev. D 86, 112007 (2012).

[47] B. Abelev et al. (ALICE Collaboration), Beauty production in pp collisions at $\sqrt{s} = 2.76$ TeV measured via semi-electronic decays, Phys. Lett. B 738, 97 (2014).

[48] S. Roesler, R. Engel, and J. Ranft, The Monte Carlo event generator DPMJET-III, in Advanced Monte Carlo for radiation physics, particle transport simulation and

applications. *Proceedings, Conference, MC2000, Lisbon, Portugal, 2000* (Springer, Berlin, 2000), pp. 1033–1038.

[49] S. S. Adler *et al.* (PHENIX Collaboration), Dense-Medium Modifications to Jet-Induced Hadron Pair Distributions in Au + Au Collisions at $\sqrt{s_{NN}} = 200$ GeV, Phys. Rev. Lett. **97**, 052301 (2006).

[50] B. Abelev *et al.* (ALICE Collaboration), Transverse Momentum Distribution and Nuclear Modification Factor of Charged Particles in *p*-Pb Collisions at $\sqrt{s_{NN}} = 5.02$ TeV, Phys. Rev. Lett. **110**, 082302 (2013).

S. Acharya,[139] D. Adamová,[93] J. Adolfsson,[80] M. M. Aggarwal,[98] G. Aglieri Rinella,[34] M. Agnello,[31] N. Agrawal,[48] Z. Ahammed,[139] S. U. Ahn,[76] S. Aiola,[144] A. Akindinov,[64] M. Al-Turany,[104] S. N. Alam,[139] D. S. D. Albuquerque,[121] D. Aleksandrov,[87] B. Alessandro,[58] R. Alfaro Molina,[72] Y. Ali,[15] A. Alici,[10,53,27] A. Alkin,[2] J. Alme,[22] T. Alt,[69] L. Altenkamper,[22] I. Altsybeev,[111] M. N. Anaam,[6] C. Andrei,[47] D. Andreou,[34] H. A. Andrews,[108] A. Andronic,[142,104] M. Angeletti,[34] V. Anguelov,[102] C. Anson,[16] T. Antičić,[105] F. Antinori,[56] P. Antonioli,[53] R. Anwar,[125] N. Apadula,[79] L. Aphecetche,[113] H. Appelshäuser,[69] S. Arcelli,[27] R. Arnaldi,[58] O. W. Arnold,[103,116] I. C. Arsene,[21] M. Arslandok,[102] A. Augustinus,[34] R. Averbeck,[104] M. D. Azmi,[17] A. Badalà,[55] Y. W. Baek,[60,40] S. Bagnasco,[58] R. Bailhache,[69] R. Bala,[99] A. Baldisseri,[135] M. Ball,[42] R. C. Baral,[85] A. M. Barbano,[26] R. Barbera,[28] F. Barile,[52] L. Barioglio,[26] G. G. Barnaföldi,[143] L. S. Barnby,[92] V. Barret,[132] P. Bartalini,[6] K. Barth,[34] E. Bartsch,[69] N. Bastid,[132] S. Basu,[141] G. Batigne,[113] B. Batyunya,[75] P. C. Batzing,[21] J. L. Bazo Alba,[109] I. G. Bearden,[88] H. Beck,[102] C. Bedda,[63] N. K. Behera,[60] I. Belikov,[134] F. Bellini,[34] H. Bello Martinez,[44] R. Bellwied,[125] L. G. E. Beltran,[119] V. Belyaev,[91] G. Bencedi,[143] S. Beole,[26] A. Bercuci,[47] Y. Berdnikov,[96] D. Berenyi,[143] R. A. Bertens,[128] D. Berzano,[34,58] L. Betev,[34] P. P. Bhaduri,[139] A. Bhasin,[99] I. R. Bhat,[99] H. Bhatt,[48] B. Bhattacharjee,[41] J. Bhom,[117] A. Bianchi,[26] L. Bianchi,[125] N. Bianchi,[51] J. Bielčík,[37] J. Bielčíková,[93] A. Bilandzic,[116,103] G. Biro,[143] R. Biswas,[3] S. Biswas,[3] J. T. Blair,[118] D. Blau,[87] C. Blume,[69] G. Boca,[137] F. Bock,[34] A. Bogdanov,[91] L. Boldizsár,[143] M. Bombara,[38] G. Bonomi,[138] M. Bonora,[34] H. Borel,[135] A. Borissov,[142] M. Borri,[127] E. Botta,[26] C. Bourjau,[88] L. Bratrud,[69] P. Braun-Munzinger,[104] M. Bregant,[120] T. A. Broker,[69] M. Broz,[37] E. J. Brucken,[43] E. Bruna,[58] G. E. Bruno,[34,33] D. Budnikov,[106] H. Buesching,[69] S. Bufalino,[31] P. Buhler,[112] P. Buncic,[34] O. Busch,[131,†] Z. Buthelezi,[73] J. B. Butt,[15] J. T. Buxton,[95] J. Cabala,[115] D. Caffarri,[89] H. Caines,[144] A. Caliva,[104] E. Calvo Villar,[109] R. S. Camacho,[44] P. Camerini,[25] A. A. Capon,[112] F. Carena,[34] W. Carena,[34] F. Carnesecchi,[27,10] J. Castillo Castellanos,[135] A. J. Castro,[128] E. A. R. Casula,[54] C. Ceballos Sanchez,[8] S. Chandra,[139] B. Chang,[126] W. Chang,[6] S. Chapeland,[34] M. Chartier,[127] S. Chattopadhyay,[139] S. Chattopadhyay,[107] A. Chauvin,[103,116] C. Cheshkov,[133] B. Cheynis,[133] V. Chibante Barroso,[34] D. D. Chinellato,[121] S. Cho,[60] P. Chochula,[34] T. Chowdhury,[132] P. Christakoglou,[89] C. H. Christensen,[88] P. Christiansen,[80] T. Chujo,[131] S. U. Chung,[18] C. Cicalo,[54] L. Cifarelli,[10,27] F. Cindolo,[53] J. Cleymans,[124] F. Colamaria,[52] D. Colella,[65,52] A. Collu,[79] M. Colocci,[27] M. Concas,[58,a] G. Conesa Balbastre,[78] Z. Conesa del Valle,[61] J. G. Contreras,[37] T. M. Cormier,[94] Y. Corrales Morales,[58] P. Cortese,[32] M. R. Cosentino,[122] F. Costa,[34] S. Costanza,[137] J. Crkovská,[61] P. Crochet,[132] E. Cuautle,[70] L. Cunqueiro,[142,94] T. Dahms,[103,116] A. Dainese,[56] S. Dani,[66] M. C. Danisch,[102] A. Danu,[68] D. Das,[107] I. Das,[107] S. Das,[3] A. Dash,[85] S. Dash,[48] S. De,[49] A. De Caro,[30] G. de Cataldo,[52] C. de Conti,[120] J. de Cuveland,[39] A. De Falco,[24] D. De Gruttola,[10,30] N. De Marco,[58] S. De Pasquale,[30] R. D. De Souza,[121] H. F. Degenhardt,[120] A. Deisting,[104,102] A. Deloff,[84] S. Delsanto,[26] C. Deplano,[89] P. Dhankher,[48] D. Di Bari,[33] A. Di Mauro,[34] B. Di Ruzza,[56] R. A. Diaz,[8] T. Dietel,[124] P. Dillenseger,[69] Y. Ding,[6] R. Divià,[34] Ø. Djuvsland,[22] A. Dobrin,[34] D. Domenicis Gimenez,[120] B. Dönigus,[69] O. Dordic,[21] L. V. R. Doremalen,[63] A. K. Dubey,[139] A. Dubla,[104] L. Ducroux,[133] S. Dudi,[98] A. K. Duggal,[98] M. Dukhishyam,[85] P. Dupieux,[132] R. J. Ehlers,[144] D. Elia,[52] E. Endress,[109] H. Engel,[74] E. Epple,[144] B. Erazmus,[113] F. Erhardt,[97] M. R. Ersdal,[22] B. Espagnon,[61] G. Eulisse,[34] J. Eum,[18] D. Evans,[108] S. Evdokimov,[90] L. Fabbietti,[103,116] M. Faggin,[29] J. Faivre,[78] A. Fantoni,[51] M. Fasel,[94] L. Feldkamp,[142] A. Feliciello,[58] G. Feofilov,[111] A. Fernández Téllez,[44] A. Ferretti,[26] A. Festanti,[34] V. J. G. Feuillard,[102] J. Figiel,[117] M. A. S. Figueredo,[120] S. Filchagin,[106] D. Finogeev,[62] F. M. Fionda,[22] G. Fiorenza,[52] F. Flor,[125] M. Floris,[34] S. Foertsch,[73] P. Foka,[104] S. Fokin,[87] E. Fragiacomo,[59] A. Francescon,[34] A. Francisco,[113] U. Frankenfeld,[104] G. G. Fronze,[26] U. Fuchs,[34] C. Furget,[78] A. Furs,[62] M. Fusco Girard,[30] J. J. Gaardhøje,[88] M. Gagliardi,[26] A. M. Gago,[109] K. Gajdosova,[88] M. Gallio,[26] C. D. Galvan,[119] P. Ganoti,[83] C. Garabatos,[104] E. Garcia-Solis,[11] K. Garg,[28] C. Gargiulo,[34] P. Gasik,[116,103] E. F. Gauger,[118] M. B. Gay Ducati,[71] M. Germain,[113] J. Ghosh,[107] P. Ghosh,[139] S. K. Ghosh,[3] P. Gianotti,[51] P. Giubellino,[104,58] P. Giubilato,[29] P. Glässel,[102] D. M. Gomez Coral,[72] A. Gomez Ramirez,[74] V. Gonzalez,[104] P. González-Zamora,[44] S. Gorbunov,[39]

L. Görlich,[117] S. Gotovac,[35] V. Grabski,[72] L. K. Graczykowski,[140] K. L. Graham,[108] L. Greiner,[79] A. Grelli,[63] C. Grigoras,[34] V. Grigoriev,[91] A. Grigoryan,[1] S. Grigoryan,[75] J. M. Gronefeld,[104] F. Grosa,[31] J. F. Grosse-Oetringhaus,[34] R. Grosso,[104] R. Guernane,[78] B. Guerzoni,[27] M. Guittiere,[113] K. Gulbrandsen,[88] T. Gunji,[130] A. Gupta,[99] R. Gupta,[99] I. B. Guzman,[44] R. Haake,[34] M. K. Habib,[104] C. Hadjidakis,[61] H. Hamagaki,[81] G. Hamar,[143] M. Hamid,[6] J. C. Hamon,[134] R. Hannigan,[118] M. R. Haque,[63] A. Harlenderova,[104] J. W. Harris,[144] A. Harton,[11] H. Hassan,[78] D. Hatzifotiadou,[53,10] S. Hayashi,[130] S. T. Heckel,[69] E. Hellbär,[69] H. Helstrup,[36] A. Herghelegiu,[47] E. G. Hernandez,[44] G. Herrera Corral,[9] F. Herrmann,[142] K. F. Hetland,[36] T. E. Hilden,[43] H. Hillemanns,[34] C. Hills,[127] B. Hippolyte,[134] B. Hohlweger,[103] D. Horak,[37] S. Hornung,[104] R. Hosokawa,[131,78] J. Hota,[66] P. Hristov,[34] C. Huang,[61] C. Hughes,[128] P. Huhn,[69] T. J. Humanic,[95] H. Hushnud,[107] N. Hussain,[41] T. Hussain,[17] D. Hutter,[39] D. S. Hwang,[19] J. P. Iddon,[127] S. A. Iga Buitron,[70] R. Ilkaev,[106] M. Inaba,[131] M. Ippolitov,[87] M. S. Islam,[107] M. Ivanov,[104] V. Ivanov,[96] V. Izucheev,[90] B. Jacak,[79] N. Jacazio,[27] P. M. Jacobs,[79] M. B. Jadhav,[48] S. Jadlovska,[115] J. Jadlovsky,[115] S. Jaelani,[63] C. Jahnke,[120,116] M. J. Jakubowska,[140] M. A. Janik,[140] C. Jena,[85] M. Jercic,[97] O. Jevons,[108] R. T. Jimenez Bustamante,[104] M. Jin,[125] P. G. Jones,[108] A. Jusko,[108] P. Kalinak,[65] A. Kalweit,[34] J. H. Kang,[145] V. Kaplin,[91] S. Kar,[6] A. Karasu Uysal,[77] O. Karavichev,[62] T. Karavicheva,[62] P. Karczmarczyk,[34] E. Karpechev,[62] U. Kebschull,[74] R. Keidel,[46] D. L. D. Keijdener,[63] M. Keil,[34] B. Ketzer,[42] Z. Khabanova,[89] A. M. Khan,[6] S. Khan,[17] S. A. Khan,[139] A. Khanzadeev,[96] Y. Kharlov,[90] A. Khatun,[17] A. Khuntia,[49] M. M. Kielbowicz,[117] B. Kileng,[36] B. Kim,[131] D. Kim,[145] D. J. Kim,[126] E. J. Kim,[13] H. Kim,[145] J. S. Kim,[40] J. Kim,[102] M. Kim,[102,60] S. Kim,[19] T. Kim,[145] T. Kim,[145] S. Kirsch,[39] I. Kisel,[39] S. Kiselev,[64] A. Kisiel,[140] J. L. Klay,[5] C. Klein,[69] J. Klein,[34,58] C. Klein-Bösing,[142] S. Klewin,[102] A. Kluge,[34] M. L. Knichel,[34] A. G. Knospe,[125] C. Kobdaj,[114] M. Kofarago,[143] M. K. Köhler,[102] T. Kollegger,[104] N. Kondratyeva,[91] E. Kondratyuk,[90] A. Konevskikh,[62] P. J. Konopka,[34] M. Konyushikhin,[141] O. Kovalenko,[84] V. Kovalenko,[111] M. Kowalski,[117] I. Králik,[65] A. Kravčáková,[38] L. Kreis,[104] M. Krivda,[65,108] F. Krizek,[93] M. Krüger,[69] E. Kryshen,[96] M. Krzewicki,[39] A. M. Kubera,[95] V. Kučera,[60,93] C. Kuhn,[134] P. G. Kuijer,[89] J. Kumar,[48] L. Kumar,[98] S. Kumar,[48] S. Kundu,[85] P. Kurashvili,[84] A. Kurepin,[62] A. B. Kurepin,[62] A. Kuryakin,[106] S. Kushpil,[93] J. Kvapil,[108] M. J. Kweon,[60] Y. Kwon,[145] S. L. La Pointe,[39] P. La Rocca,[28] Y. S. Lai,[79] I. Lakomov,[34] R. Langoy,[123] K. Lapidus,[144] A. Lardeux,[21] P. Larionov,[51] E. Laudi,[34] R. Lavicka,[37] R. Lea,[25] L. Leardini,[102] S. Lee,[145] F. Lehas,[89] S. Lehner,[112] J. Lehrbach,[39] R. C. Lemmon,[92] I. León Monzón,[119] P. Lévai,[143] X. Li,[12] X. L. Li,[6] J. Lien,[123] R. Lietava,[108] B. Lim,[18] S. Lindal,[21] V. Lindenstruth,[39] S. W. Lindsay,[127] C. Lippmann,[104] M. A. Lisa,[95] V. Litichevskyi,[43] A. Liu,[79] H. M. Ljunggren,[80] W. J. Llope,[141] D. F. Lodato,[63] V. Loginov,[91] C. Loizides,[94,79] P. Loncar,[35] X. Lopez,[132] E. López Torres,[8] A. Lowe,[143] P. Luettig,[69] J. R. Luhder,[142] M. Lunardon,[29] G. Luparello,[59] M. Lupi,[34] A. Maevskaya,[62] M. Mager,[34] S. M. Mahmood,[21] A. Maire,[134] R. D. Majka,[144] M. Malaev,[96] Q. W. Malik,[21] L. Malinina,[75,b] D. Mal'Kevich,[64] P. Malzacher,[104] A. Mamonov,[106] V. Manko,[87] F. Manso,[132] V. Manzari,[52] Y. Mao,[6] M. Marchisone,[129,73,133] J. Mareš,[67] G. V. Margagliotti,[25] A. Margotti,[53] J. Margutti,[63] A. Marín,[104] C. Markert,[118] M. Marquard,[69] N. A. Martin,[104] P. Martinengo,[34] J. L. Martinez,[125] M. I. Martínez,[44] G. Martínez García,[113] M. Martinez Pedreira,[34] S. Masciocchi,[104] M. Masera,[26] A. Masoni,[54] L. Massacrier,[61] E. Masson,[113] A. Mastroserio,[52,136] A. M. Mathis,[116,103] P. F. T. Matuoka,[120] A. Matyja,[117,128] C. Mayer,[117] M. Mazzilli,[33] M. A. Mazzoni,[57] F. Meddi,[23] Y. Melikyan,[91] A. Menchaca-Rocha,[72] E. Meninno,[30] J. Mercado Pérez,[102] M. Meres,[14] C. S. Meza,[109] S. Mhlanga,[124] Y. Miake,[131] L. Micheletti,[26] M. M. Mieskolainen,[43] D. L. Mihaylov,[103] K. Mikhaylov,[64,75] A. Mischke,[63] A. N. Mishra,[70] D. Miśkowiec,[104] J. Mitra,[139] C. M. Mitu,[68] N. Mohammadi,[34] A. P. Mohanty,[63] B. Mohanty,[85] M. Mohisin Khan,[17,c] D. A. Moreira De Godoy,[142] L. A. P. Moreno,[44] S. Moretto,[29] A. Morreale,[113] A. Morsch,[34] T. Mrnjavac,[34] V. Muccifora,[51] E. Mudnic,[35] D. Mühlheim,[142] S. Muhuri,[139] M. Mukherjee,[3] J. D. Mulligan,[144] M. G. Munhoz,[120] K. Münning,[42] M. I. A. Munoz,[79] R. H. Munzer,[69] H. Murakami,[130] S. Murray,[73] L. Musa,[34] J. Musinsky,[65] C. J. Myers,[125] J. W. Myrcha,[140] B. Naik,[48] R. Nair,[84] B. K. Nandi,[48] R. Nania,[53,10] E. Nappi,[52] A. Narayan,[48] M. U. Naru,[15] A. F. Nassirpour,[80] H. Natal da Luz,[120] C. Nattrass,[128] S. R. Navarro,[44] K. Nayak,[85] R. Nayak,[48] T. K. Nayak,[139] S. Nazarenko,[106] R. A. Negrao De Oliveira,[69,34] L. Nellen,[70] S. V. Nesbo,[36] G. Neskovic,[39] F. Ng,[125] M. Nicassio,[104] J. Niedziela,[140,34] B. S. Nielsen,[88] S. Nikolaev,[87] S. Nikulin,[87] V. Nikulin,[96] F. Noferini,[10,53] P. Nomokonov,[75] G. Nooren,[63] J. C. C. Noris,[44] J. Norman,[78] A. Nyanin,[87] J. Nystrand,[22] H. Oh,[145] A. Ohlson,[102] J. Oleniacz,[140] A. C. Oliveira Da Silva,[120] M. H. Oliver,[144] J. Onderwaater,[104] C. Oppedisano,[58] R. Orava,[43] M. Oravec,[115] A. Ortiz Velasquez,[70] A. Oskarsson,[80] J. Otwinowski,[117] K. Oyama,[81] Y. Pachmayer,[102] V. Pacik,[88] D. Pagano,[138] G. Paić,[70] P. Palni,[6] J. Pan,[141] A. K. Pandey,[48] S. Panebianco,[135] V. Papikyan,[1] P. Pareek,[49] J. Park,[60] J. E. Parkkila,[126] S. Parmar,[98] A. Passfeld,[142] S. P. Pathak,[125] R. N. Patra,[139] B. Paul,[58] H. Pei,[6] T. Peitzmann,[63] X. Peng,[6] L. G. Pereira,[71] H. Pereira Da Costa,[135] D. Peresunko,[87] E. Perez Lezama,[69] V. Peskov,[69] Y. Pestov,[4] V. Petráček,[37]

M. Petrovici,[47] C. Petta,[28] R. P. Pezzi,[71] S. Piano,[59] M. Pikna,[14] P. Pillot,[113] L. O. D. L. Pimentel,[88] O. Pinazza,[53,34] L. Pinsky,[125] S. Pisano,[51] D. B. Piyarathna,[125] M. Płoskoń,[79] M. Planinic,[97] F. Pliquett,[69] J. Pluta,[140] S. Pochybova,[143] P. L. M. Podesta-Lerma,[119] M. G. Poghosyan,[94] B. Polichtchouk,[90] N. Poljak,[97] W. Poonsawat,[114] A. Pop,[47] H. Poppenborg,[142] S. Porteboeuf-Houssais,[132] V. Pozdniakov,[75] S. K. Prasad,[3] R. Preghenella,[53] F. Prino,[58] C. A. Pruneau,[141] I. Pshenichnov,[62] M. Puccio,[26] V. Punin,[106] J. Putschke,[141] S. Raha,[3] S. Rajput,[99] J. Rak,[126] A. Rakotozafindrabe,[135] L. Ramello,[32] F. Rami,[134] R. Raniwala,[100] S. Raniwala,[100] S. S. Räsänen,[43] B. T. Rascanu,[69] V. Ratza,[42] I. Ravasenga,[31] K. F. Read,[128,94] K. Redlich,[84,d] A. Rehman,[22] P. Reichelt,[69] F. Reidt,[34] X. Ren,[6] R. Renfordt,[69] A. Reshetin,[62] J.-P. Revol,[10] K. Reygers,[102] V. Riabov,[96] T. Richert,[63] M. Richter,[21] P. Riedler,[34] W. Riegler,[34] F. Riggi,[28] C. Ristea,[68] S. P. Rode,[49] M. Rodríguez Cahuantzi,[44] K. Røed,[21] R. Rogalev,[90] E. Rogochaya,[75] D. Rohr,[34] D. Röhrich,[22] P. S. Rokita,[140] F. Ronchetti,[51] E. D. Rosas,[70] K. Roslon,[140] P. Rosnet,[132] A. Rossi,[29] A. Rotondi,[137] F. Roukoutakis,[83] C. Roy,[134] P. Roy,[107] O. V. Rueda,[70] R. Rui,[25] B. Rumyantsev,[75] A. Rustamov,[86] E. Ryabinkin,[87] Y. Ryabov,[96] A. Rybicki,[117] S. Saarinen,[43] S. Sadhu,[139] S. Sadovsky,[90] K. Šafařík,[34] S. K. Saha,[139] B. Sahoo,[48] P. Sahoo,[49] R. Sahoo,[49] S. Sahoo,[66] P. K. Sahu,[66] J. Saini,[139] S. Sakai,[131] M. A. Saleh,[141] S. Sambyal,[99] V. Samsonov,[96,91] A. Sandoval,[72] A. Sarkar,[73] D. Sarkar,[139] N. Sarkar,[139] P. Sarma,[41] M. H. P. Sas,[63] E. Scapparone,[53] F. Scarlassara,[29] B. Schaefer,[94] H. S. Scheid,[69] C. Schiaua,[47] R. Schicker,[102] C. Schmidt,[104] H. R. Schmidt,[101] M. O. Schmidt,[102] M. Schmidt,[101] N. V. Schmidt,[94,69] J. Schukraft,[34] Y. Schutz,[34,134] K. Schwarz,[104] K. Schweda,[104] G. Scioli,[27] E. Scomparin,[58] M. Šefčík,[38] J. E. Seger,[16] Y. Sekiguchi,[130] D. Sekihata,[45] I. Selyuzhenkov,[104,91] S. Senyukov,[134] E. Serradilla,[72] P. Sett,[48] A. Sevcenco,[68] A. Shabanov,[62] A. Shabetai,[113] R. Shahoyan,[34] W. Shaikh,[107] A. Shangaraev,[90] A. Sharma,[98] A. Sharma,[99] M. Sharma,[99] N. Sharma,[98] A. I. Sheikh,[139] K. Shigaki,[45] M. Shimomura,[82] S. Shirinkin,[64] Q. Shou,[6,110] K. Shtejer,[26] Y. Sibiriak,[87] S. Siddhanta,[54] K. M. Sielewicz,[34] T. Siemiarczuk,[84] D. Silvermyr,[80] G. Simatovic,[89] G. Simonetti,[34,103] R. Singaraju,[139] R. Singh,[85] R. Singh,[99] V. Singhal,[139] T. Sinha,[107] B. Sitar,[14] M. Sitta,[32] T. B. Skaali,[21] M. Slupecki,[126] N. Smirnov,[144] R. J. M. Snellings,[63] T. W. Snellman,[126] J. Song,[18] F. Soramel,[29] S. Sorensen,[128] F. Sozzi,[104] I. Sputowska,[117] J. Stachel,[102] I. Stan,[68] P. Stankus,[94] E. Stenlund,[80] D. Stocco,[113] M. M. Storetvedt,[36] P. Strmen,[14] A. A. P. Suaide,[120] T. Sugitate,[45] C. Suire,[61] M. Suleymanov,[15] M. Suljic,[34,25] R. Sultanov,[64] M. Šumbera,[93] S. Sumowidagdo,[50] K. Suzuki,[112] S. Swain,[66] A. Szabo,[14] I. Szarka,[14] U. Tabassam,[15] J. Takahashi,[121] G. J. Tambave,[22] N. Tanaka,[131] M. Tarhini,[113] M. Tariq,[17] M. G. Tarzila,[47] A. Tauro,[34] G. Tejeda Muñoz,[44] A. Telesca,[34] C. Terrevoli,[29] B. Teyssier,[133] D. Thakur,[49] S. Thakur,[139] D. Thomas,[118] F. Thoresen,[88] R. Tieulent,[133] A. Tikhonov,[62] A. R. Timmins,[125] A. Toia,[69] N. Topilskaya,[62] M. Toppi,[51] F. Torales-Acosta,[20] S. R. Torres,[119] S. Tripathy,[49] S. Trogolo,[26] G. Trombetta,[33] L. Tropp,[38] V. Trubnikov,[2] W. H. Trzaska,[126] T. P. Trzcinski,[140] B. A. Trzeciak,[63] T. Tsuji,[130] A. Tumkin,[106] R. Turrisi,[56] T. S. Tveter,[21] K. Ullaland,[22] E. N. Umaka,[125] A. Uras,[133] G. L. Usai,[24] A. Utrobicic,[97] M. Vala,[115] J. W. Van Hoorne,[34] M. van Leeuwen,[63] P. Vande Vyvre,[34] D. Varga,[143] A. Vargas,[44] M. Vargyas,[126] R. Varma,[48] M. Vasileiou,[83] A. Vasiliev,[87] A. Vauthier,[78] O. Vázquez Doce,[103,116] V. Vechernin,[111] A. M. Veen,[63] E. Vercellin,[26] S. Vergara Limón,[44] L. Vermunt,[63] R. Vernet,[7] R. Vértesi,[143] L. Vickovic,[35] J. Viinikainen,[126] Z. Vilakazi,[129] O. Villalobos Baillie,[108] A. Villatoro Tello,[44] A. Vinogradov,[87] T. Virgili,[30] V. Vislavicius,[88,80] A. Vodopyanov,[75] M. A. Völkl,[101] K. Voloshin,[64] S. A. Voloshin,[141] G. Volpe,[33] B. von Haller,[34] I. Vorobyev,[116,103] D. Voscek,[115] D. Vranic,[104,34] J. Vrláková,[38] B. Wagner,[22] H. Wang,[63] M. Wang,[6] Y. Watanabe,[131] M. Weber,[112] S. G. Weber,[104] A. Wegrzynek,[34] D. F. Weiser,[102] S. C. Wenzel,[34] J. P. Wessels,[142] U. Westerhoff,[142] A. M. Whitehead,[124] J. Wiechula,[69] J. Wikne,[21] G. Wilk,[84] J. Wilkinson,[53] G. A. Willems,[142,34] M. C. S. Williams,[53] E. Willsher,[108] B. Windelband,[102] W. E. Witt,[128] R. Xu,[6] S. Yalcin,[77] K. Yamakawa,[45] S. Yano,[45] Z. Yin,[6] H. Yokoyama,[78,131] I.-K. Yoo,[18] J. H. Yoon,[60] V. Yurchenko,[2] V. Zaccolo,[58] A. Zaman,[15] C. Zampolli,[34] H. J. C. Zanoli,[120] N. Zardoshti,[108] A. Zarochentsev,[111] P. Závada,[67] N. Zaviyalov,[106] H. Zbroszczyk,[140] M. Zhalov,[96] X. Zhang,[6] Y. Zhang,[6] Z. Zhang,[6,132] C. Zhao,[21] V. Zherebchevskii,[111] N. Zhigareva,[64] D. Zhou,[6] Y. Zhou,[88] Z. Zhou,[22] H. Zhu,[6] J. Zhu,[6] Y. Zhu,[6] A. Zichichi,[27,10] M. B. Zimmermann,[34] G. Zinovjev,[2] J. Zmeskal,[112] and S. Zou[6]

(ALICE Collaboration)

[1]A.I. Alikhanyan National Science Laboratory (Yerevan Physics Institute) Foundation, Yerevan, Armenia
[2]Bogolyubov Institute for Theoretical Physics, National Academy of Sciences of Ukraine, Kiev, Ukraine
[3]Bose Institute, Department of Physics and Centre for Astroparticle Physics and Space Science (CAPSS), Kolkata, India
[4]Budker Institute for Nuclear Physics, Novosibirsk, Russia

[5]*California Polytechnic State University, San Luis Obispo, California, USA*
[6]*Central China Normal University, Wuhan, China*
[7]*Centre de Calcul de l'IN2P3, Villeurbanne, Lyon, France*
[8]*Centro de Aplicaciones Tecnológicas y Desarrollo Nuclear (CEADEN), Havana, Cuba*
[9]*Centro de Investigación y de Estudios Avanzados (CINVESTAV), Mexico City and Mérida, Mexico*
[10]*Centro Fermi - Museo Storico della Fisica e Centro Studi e Ricerche "Enrico Fermi", Rome, Italy*
[11]*Chicago State University, Chicago, Illinois, USA*
[12]*China Institute of Atomic Energy, Beijing, China*
[13]*Chonbuk National University, Jeonju, Republic of Korea*
[14]*Comenius University Bratislava, Faculty of Mathematics, Physics and Informatics, Bratislava, Slovakia*
[15]*COMSATS Institute of Information Technology (CIIT), Islamabad, Pakistan*
[16]*Creighton University, Omaha, Nebraska, USA*
[17]*Department of Physics, Aligarh Muslim University, Aligarh, India*
[18]*Department of Physics, Pusan National University, Pusan, Republic of Korea*
[19]*Department of Physics, Sejong University, Seoul, Republic of Korea*
[20]*Department of Physics, University of California, Berkeley, California, USA*
[21]*Department of Physics, University of Oslo, Oslo, Norway*
[22]*Department of Physics and Technology, University of Bergen, Bergen, Norway*
[23]*Dipartimento di Fisica dell'Università "La Sapienza" and Sezione INFN, Rome, Italy*
[24]*Dipartimento di Fisica dell'Università and Sezione INFN, Cagliari, Italy*
[25]*Dipartimento di Fisica dell'Università and Sezione INFN, Trieste, Italy*
[26]*Dipartimento di Fisica dell'Università and Sezione INFN, Turin, Italy*
[27]*Dipartimento di Fisica e Astronomia dell'Università and Sezione INFN, Bologna, Italy*
[28]*Dipartimento di Fisica e Astronomia dell'Università and Sezione INFN, Catania, Italy*
[29]*Dipartimento di Fisica e Astronomia dell'Università and Sezione INFN, Padova, Italy*
[30]*Dipartimento di Fisica "E.R. Caianiello" dell'Università and Gruppo Collegato INFN, Salerno, Italy*
[31]*Dipartimento DISAT del Politecnico and Sezione INFN, Turin, Italy*
[32]*Dipartimento di Scienze e Innovazione Tecnologica dell'Università del Piemonte Orientale and INFN Sezione di Torino, Alessandria, Italy*
[33]*Dipartimento Interateneo di Fisica "M. Merlin" and Sezione INFN, Bari, Italy*
[34]*European Organization for Nuclear Research (CERN), Geneva, Switzerland*
[35]*Faculty of Electrical Engineering, Mechanical Engineering and Naval Architecture, University of Split, Split, Croatia*
[36]*Faculty of Engineering and Science, Western Norway University of Applied Sciences, Bergen, Norway*
[37]*Faculty of Nuclear Sciences and Physical Engineering, Czech Technical University in Prague, Prague, Czech Republic*
[38]*Faculty of Science, P.J. Šafárik University, Košice, Slovakia*
[39]*Frankfurt Institute for Advanced Studies, Johann Wolfgang Goethe-Universität Frankfurt, Frankfurt, Germany*
[40]*Gangneung-Wonju National University, Gangneung, Republic of Korea*
[41]*Gauhati University, Department of Physics, Guwahati, India*
[42]*Helmholtz-Institut für Strahlen- und Kernphysik, Rheinische Friedrich-Wilhelms-Universität Bonn, Bonn, Germany*
[43]*Helsinki Institute of Physics (HIP), Helsinki, Finland*
[44]*High Energy Physics Group, Universidad Autónoma de Puebla, Puebla, Mexico*
[45]*Hiroshima University, Hiroshima, Japan*
[46]*Hochschule Worms, Zentrum für Technologietransfer und Telekommunikation (ZTT), Worms, Germany*
[47]*Horia Hulubei National Institute of Physics and Nuclear Engineering, Bucharest, Romania*
[48]*Indian Institute of Technology Bombay (IIT), Mumbai, India*
[49]*Indian Institute of Technology Indore, Indore, India*
[50]*Indonesian Institute of Sciences, Jakarta, Indonesia*
[51]*INFN, Laboratori Nazionali di Frascati, Frascati, Italy*
[52]*INFN, Sezione di Bari, Bari, Italy*
[53]*INFN, Sezione di Bologna, Bologna, Italy*
[54]*INFN, Sezione di Cagliari, Cagliari, Italy*
[55]*INFN, Sezione di Catania, Catania, Italy*
[56]*INFN, Sezione di Padova, Padova, Italy*
[57]*INFN, Sezione di Roma, Rome, Italy*
[58]*INFN, Sezione di Torino, Turin, Italy*
[59]*INFN, Sezione di Trieste, Trieste, Italy*
[60]*Inha University, Incheon, Republic of Korea*
[61]*Institut de Physique Nucléaire d'Orsay (IPNO), Institut National de Physique Nucléaire et de Physique des Particules (IN2P3/CNRS), Université de Paris-Sud, Université Paris-Saclay, Orsay, France*
[62]*Institute for Nuclear Research, Academy of Sciences, Moscow, Russia*

[63]Institute for Subatomic Physics, Utrecht University/Nikhef, Utrecht, Netherlands

[64]Institute for Theoretical and Experimental Physics, Moscow, Russia

[65]Institute of Experimental Physics, Slovak Academy of Sciences, Košice, Slovakia

[66]Institute of Physics, Homi Bhabha National Institute, Bhubaneswar, India

[67]Institute of Physics of the Czech Academy of Sciences, Prague, Czech Republic

[68]Institute of Space Science (ISS), Bucharest, Romania

[69]Institut für Kernphysik, Johann Wolfgang Goethe-Universität Frankfurt, Frankfurt, Germany

[70]Instituto de Ciencias Nucleares, Universidad Nacional Autónoma de México, Mexico City, Mexico

[71]Instituto de Física, Universidade Federal do Rio Grande do Sul (UFRGS), Porto Alegre, Brazil

[72]Instituto de Física, Universidad Nacional Autónoma de México, Mexico City, Mexico

[73]iThemba LABS, National Research Foundation, Somerset West, South Africa

[74]Johann-Wolfgang-Goethe Universität Frankfurt Institut für Informatik, Fachbereich Informatik und Mathematik, Frankfurt, Germany

[75]Joint Institute for Nuclear Research (JINR), Dubna, Russia

[76]Korea Institute of Science and Technology Information, Daejeon, Republic of Korea

[77]KTO Karatay University, Konya, Turkey

[78]Laboratoire de Physique Subatomique et de Cosmologie, Université Grenoble-Alpes, CNRS-IN2P3, Grenoble, France

[79]Lawrence Berkeley National Laboratory, Berkeley, California, USA

[80]Lund University Department of Physics, Division of Particle Physics, Lund, Sweden

[81]Nagasaki Institute of Applied Science, Nagasaki, Japan

[82]Nara Women's University (NWU), Nara, Japan

[83]National and Kapodistrian University of Athens, School of Science, Department of Physics, Athens, Greece

[84]National Centre for Nuclear Research, Warsaw, Poland

[85]National Institute of Science Education and Research, Homi Bhabha National Institute, Jatni, India

[86]National Nuclear Research Center, Baku, Azerbaijan

[87]National Research Centre Kurchatov Institute, Moscow, Russia

[88]Niels Bohr Institute, University of Copenhagen, Copenhagen, Denmark

[89]Nikhef, National institute for subatomic physics, Amsterdam, Netherlands

[90]NRC Kurchatov Institute IHEP, Protvino, Russia

[91]NRNU Moscow Engineering Physics Institute, Moscow, Russia

[92]Nuclear Physics Group, STFC Daresbury Laboratory, Daresbury, United Kingdom

[93]Nuclear Physics Institute of the Czech Academy of Sciences, Řež u Prahy, Czech Republic

[94]Oak Ridge National Laboratory, Oak Ridge, Tennessee, USA

[95]Ohio State University, Columbus, Ohio, USA

[96]Petersburg Nuclear Physics Institute, Gatchina, Russia

[97]Physics department, Faculty of science, University of Zagreb, Zagreb, Croatia

[98]Physics Department, Panjab University, Chandigarh, India

[99]Physics Department, University of Jammu, Jammu, India

[100]Physics Department, University of Rajasthan, Jaipur, India

[101]Physikalisches Institut, Eberhard-Karls-Universität Tübingen, Tübingen, Germany

[102]Physikalisches Institut, Ruprecht-Karls-Universität Heidelberg, Heidelberg, Germany

[103]Physik Department, Technische Universität München, Munich, Germany

[104]Research Division and ExtreMe Matter Institute EMMI, GSI Helmholtzzentrum für Schwerionenforschung GmbH, Darmstadt, Germany

[105]Rudjer Bošković Institute, Zagreb, Croatia

[106]Russian Federal Nuclear Center (VNIIEF), Sarov, Russia

[107]Saha Institute of Nuclear Physics, Homi Bhabha National Institute, Kolkata, India

[108]School of Physics and Astronomy, University of Birmingham, Birmingham, United Kingdom

[109]Sección Física, Departamento de Ciencias, Pontificia Universidad Católica del Perú, Lima, Peru

[110]Shanghai Institute of Applied Physics, Shanghai, China

[111]St. Petersburg State University, St. Petersburg, Russia

[112]Stefan Meyer Institut für Subatomare Physik (SMI), Vienna, Austria

[113]SUBATECH, IMT Atlantique, Université de Nantes, CNRS-IN2P3, Nantes, France

[114]Suranaree University of Technology, Nakhon Ratchasima, Thailand

[115]Technical University of Košice, Košice, Slovakia

[116]Technische Universität München, Excellence Cluster "Universe," Munich, Germany

[117]The Henryk Niewodniczanski Institute of Nuclear Physics, Polish Academy of Sciences, Cracow, Poland

[118]The University of Texas at Austin, Austin, Texas, USA

[119]Universidad Autónoma de Sinaloa, Culiacán, Mexico

[120]Universidade de São Paulo (USP), São Paulo, Brazil

[121]Universidade Estadual de Campinas (UNICAMP), Campinas, Brazil

[122]*Universidade Federal do ABC, Santo Andre, Brazil*

[123]*University College of Southeast Norway, Tonsberg, Norway*

[124]*University of Cape Town, Cape Town, South Africa*

[125]*University of Houston, Houston, Texas, USA*

[126]*University of Jyväskylä, Jyväskylä, Finland*

[127]*University of Liverpool, Liverpool, United Kingdom*

[128]*University of Tennessee, Knoxville, Tennessee, USA*

[129]*University of the Witwatersrand, Johannesburg, South Africa*

[130]*University of Tokyo, Tokyo, Japan*

[131]*University of Tsukuba, Tsukuba, Japan*

[132]*Université Clermont Auvergne, CNRS/IN2P3, LPC, Clermont-Ferrand, France*

[133]*Université de Lyon, Université Lyon 1, CNRS/IN2P3, IPN-Lyon, Villeurbanne, Lyon, France*

[134]*Université de Strasbourg, CNRS, IPHC UMR 7178, F-67000 Strasbourg, France, Strasbourg, France*

[135]*Université Paris-Saclay Centre dÉtudes de Saclay (CEA), IRFU, Department de Physique Nucléaire (DPhN), Saclay, France*

[136]*Università degli Studi di Foggia, Foggia, Italy*

[137]*Università degli Studi di Pavia, Pavia, Italy*

[138]*Università di Brescia, Brescia, Italy*

[139]*Variable Energy Cyclotron Centre, Homi Bhabha National Institute, Kolkata, India*

[140]*Warsaw University of Technology, Warsaw, Poland*

[141]*Wayne State University, Detroit, Michigan, USA*

[142]*Westfälische Wilhelms-Universität Münster, Institut für Kernphysik, Münster, Germany*

[143]*Wigner Research Centre for Physics, Hungarian Academy of Sciences, Budapest, Hungary*

[144]*Yale University, New Haven, Connecticut, USA*

[145]*Yonsei University, Seoul, Republic of Korea*

[†]Deceased.

[a]Dipartimento DET del Politecnico di Torino, Turin, Italy.

[b]M.V. Lomonosov Moscow State University, D.V. Skobeltsyn Institute of Nuclear, Physics, Moscow, Russia.

[c]Department of Applied Physics, Aligarh Muslim University, Aligarh, India.

[d]Institute of Theoretical Physics, University of Wroclaw, Poland.